AiMT Advances in Military Technology
Vol. 7, No. 2, December 2012

Spectral Angle Mapper as a Tool for Matching the Spectra in Hyperspectral Processing

F. Racek* and T. Baláž

Department of Weapon and Ammunition, University of Defence, Brno, Czech Republic

The manuscript was received on 16 July 2012 and was accepted after revision for publication on 4 October 2012.

Abstract:

The article deals with analysis of Spectral Angle Mapper (SAM) as a tool for matching the separated endmembers with pure spectra from databases. The analysis of SAM is provided in three spectral regions: VIS, IR and VIS+IR together. Three kinds of available influences are analysed: additive noise, constant offset and slant offset.

Keywords:

Hyperspectral imaging, noise, offset, spectral angle mapper.

1. Introduction

There are increasing needs to provide wideband surveillance with high-spatial resolution on the battlefield. Tactical requirements lead to utilization of electro-optical systems which will provide ISR (Intelligence, Surveillance and Reconnaissance). This potentially requires development of compact land systems capable of wide area target types surveying and automated image processing. Thus, the multispectral (MSI), hyperpectral (HSI), and ultraspectral (USI) imaging spectrometers feature the potential for a huge spreading in the range of defence applications. The development in MSI, HSI, and USI sensor and optical related technologies for ground forces, aircraft and marine and applications is expected. The applications where the development is expected in are focused on understanding of spectral phenomenology associated with natural and composite materials, creating of spectral signature libraries, automated processing and exploitation of spectral data, target and background characterization, automatic and machine assisted target and object recognition technology, hyperspectral-based target detection, tracking, and recognition, target/object and scene segmentation, MSI and HSI imaging technologies applied to the detection of landmines, surface and buried/obscured mines, etc.

* *Corresponding author: Department of Weapon and Ammunition, University of Defence, Kounicova 65, CZ-662 10 Brno, Czech Republic, phone: +420 973 445 374, E-mail: frantisek.racek@unob.cz*

2. Hyperspectral Imaging

The traditional way of taking the digital image is connected with the techniques producing the image where any pixel as a spatial coordinate is associated with scalar value. On the other hand, in the case of hyperspectral imaging (imaging spectroscopy), the scalar value associated with the spatial pixel is supplied with a vector containing the spectral information from an observed location.

The result of HSI "image" recording is a datacube. The datacube is a three-dimensional pack of spectral images of the scene containing both spatial and spectral dimensions. The illustrative interpretation of datacube is presented in Fig. 1. We can figure the HSI datacube as a set of N unique digital spectral images (with resolution $M \times K$) taken in narrow spectral band $\Delta\lambda$. It is typical for HSI systems [1], the imaging of the scene in hundreds narrow spectral bands the spectral resolution of which is on the order of 100 (centre wavelength divided by the width of the spectral band, $\lambda/\Delta\lambda$) and finally HSI spectral bands are periodical and in contact. Simply said, HSI systems measure a continuous spectrum for each image pixel. The term voxel [2] is used instead of pixel in HSI systems. Analogically to pixel, which is a 2D picture element, the voxel is a 3D datacube element. If pixel has two spatial coordinates and represents the colour or light intensity, then the voxel has two spatial coordinates and one spectral coordinate and represents some spectral characteristic (e.g. spectral reflectivity).

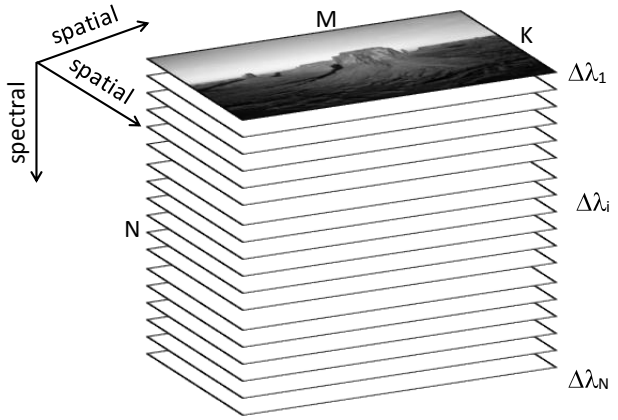

Fig. 1 HSI datacube

The amount of data in HSI datacube is huge in general. For example, a 1000 by 1000 pixel image with 100 spectral channels corresponds to a datacube with 10^8 voxels. If voxel represents 8bit digital information, the datacube size is $(10^8 \times 8)$ bits.

The complexity of HSI systems is associated with the necessity to sample the three-dimensional datacube on two-dimensional focal plane array detector. Both, to use multiple apertures or to temporally sample one of the system parameter, can be used for HSI system design. According to [3] HSI system can be classified as isomorphic systems in which each detected measurement corresponds to a specific voxel in the datacube, or multiplex systems in which each measurement corresponds to a linear combination of voxel values. Typical structure of isomorphic HSI system is presented in Fig. 2. Due to its relatively simple manufacturing, the isomorphic systems are widespread. The limitation of isomorphic systems results from their principally

low photon efficiency. The photon efficiency is decreasing with demanded high spatial and spectral resolution. Subsequently, the high spatial and spectral resolution is the cause of datacube long acquisition times and a poor signal to noise ratio (SNR).

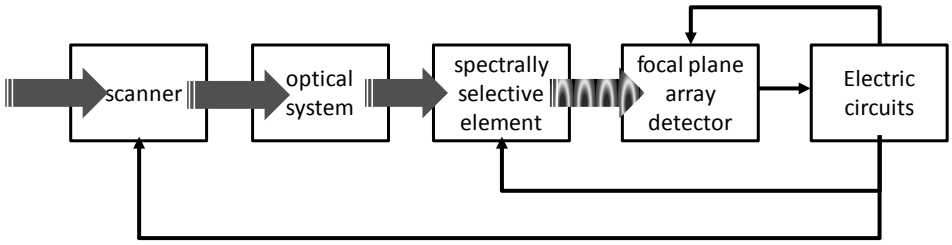

Fig. 2 HSI system

A more important feature of HSI systems from the user's point of view is the way of datacube processing. As mentioned above, datacube represents a huge amount of data; therefore the data compression is a primary part of data processing. However, it is not the focus of ordinary HSI system user, but it is to get appropriate information from the datacube. Due to rich spectral information contained in HSI datacube, the data processing is aimed to the processing of spectral characteristics of the objects inside the imagined scenery. On the contrary, the spatial pattern recognition techniques common in MSI or image processing, are in HSI assumed as a subsidiary. Thus the HSI processing is focused on the recognition of mixed spectra (mixed pixel) or the recognition of object in the scenery the dimension of which is under the spatial resolution of HSI system (subpixel).

Very roughly, the HSI processing can be divided into two fundamental steps:

- translation of radiance datacube values into the reflectance values,
- spectra matching.

Both main steps are highlighted in black colour in Fig. 3. The spectral target reflectance quality is inherent in datacube, but it is hidden in the signal affected by the conditions under which the measurement was realized. Based on the known measurement conditions (sensor quality, season, daytime, atmosphere condition, etc.), the radiance recorded in voxels can be transformed into the spectral reflectance. Next step, matching the spectra, alternates in two levels: raw spectra and mixed spectra. In the simplest case of raw spectra, the unique voxel consists of the spectrum of the single material, so-called endmember. Generally, the second case of mixed spectra is more common. Mixed spectrum occurs when more materials were in instantaneous field of view (IFOV) or radiation of recorded voxel was affected by radiation of adjacent voxel, or eventually the combination of both. The processing of mixed spectra begins with the decision whether it is mixed spectra or not. The number of endmembers is evaluated in the next step which is followed by separation of particular material spectra (unmixing). The process of unmixing is based on the assumption of either linear or nonlinear mixing model. The last step of spectra matching is finding an endmember equivalent in the spectra database [4].

3. Spectral Angle Mapper

The example of spectral reflectance data [4] is illustrated in Fig. 4. There are presented three representatives of natural materials recognizable in ordinary datacube taken in laboratory. The spectrum of a beech as an example of a vegetation spectrum of the

object with chlorophyll (such as grass, leaves, needles of conifers), the spectrum of wet clay and spectrum of sand. These spectral curves can be separated from datacube after translation of radiance into the reflectance for each image cell. These image spectra can be compared with database of laboratory reflectance spectra (so called spectral library) in order to recognize surface materials, such as particular types of vegetation, minerals or man-made materials. The Spectral Angle Mapper (SAM) [1, 5] seems to be a proper instrument for matching the endmembers with pure spectra.

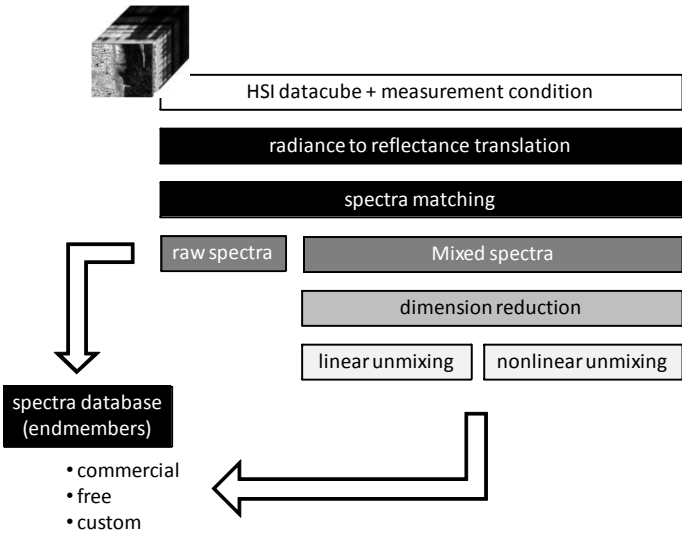

Fig. 3 Simplified model of HSI datacube processing

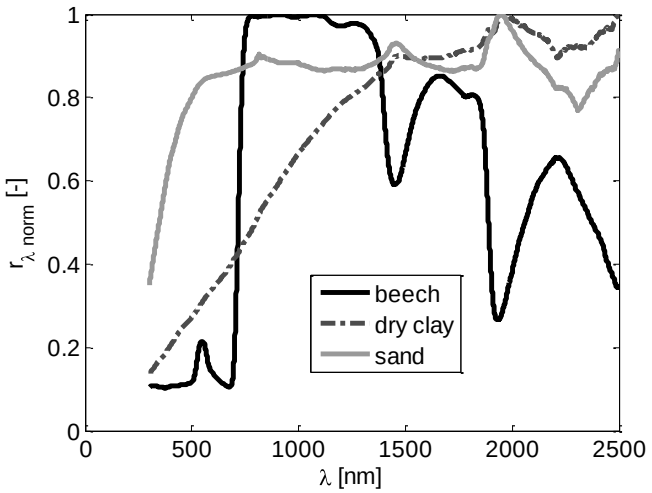

Fig. 4 Pure spectra of three representative materials: beech, dry clay and sand

The spectral reflectance data can be assumed as a distribution of reflectance data in an *n*-dimensional Euclidean space. Then, *n* is the number of spectral bands in which

the spectrum is measured. Therefore, each spectrum is assumed as a vector $\mathbf{x} = (x_1, x_2, \ldots, x_n)$. The head of the vector corresponds to a point in n-dimensional space the rectangular coordinates of which are the radiance at any spectral band. It is valid for the vector that the level of illuminance in the HSI datacube affects the length of the vector, but not its orientation. The orientation of the vector is only the function of the shape of spectral curve. Thus the orientation (angle) of the vector can be utilized as a simple and robust tool for evaluation of similarity between two spectral curves. In our case, it has been used for evaluation of similarity between the separated endmember and the pure spectra in the database.

A simple 2-band example of SAM is shown in Fig. 5. There are presented three vectors representing the spectra of materials from Fig. 4. As an example the spectra of wavelengths 550 nm for Band 1 and 1935 nm for Band 2 were selected. The reflectance values for selected bands are presented in Tab. 1.

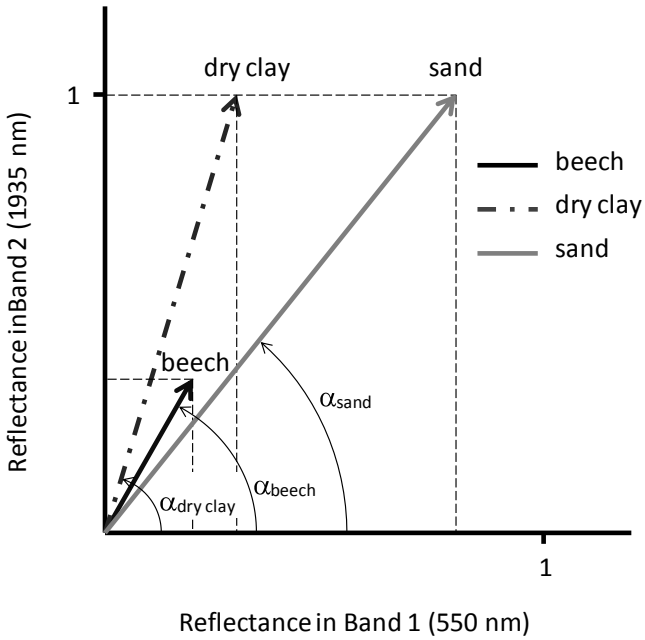

Fig. 5 2-dimensional plot of a reflectance spectrum

Tab. 1 Normalized spectral reflectance of selected materials in two spectral bands

Material	Band 1 (550 nm)	Band 2 (1935 nm)
beech	0.2	0.3
dry clay	0.3	1
sand	0.8	1

Mathematically, the vector can be characterized by its norm and angle, likewise the similarity between two spectra by the distance between two vector terminal points and angle between two vectors. The most commonly encountered vector norm, characterizing the length of the vector, is the L2-norm, given by

$$|\mathbf{v}| = \sqrt{\sum_{i=1}^{n} v_i^2} \,. \tag{1}$$

In general, the distance between heads of two vectors **x** and **y** in an Euclidean space R^n is given by

$$|\mathbf{x}-\mathbf{y}| = \sqrt{\sum_{i=1}^{n} (x_i - y_i)^2} \,. \tag{2}$$

The dot product can be defined for two vectors **x** and **y** by

$$\mathbf{x}\cdot\mathbf{y} = |\mathbf{x}||\mathbf{y}|\cos\alpha \,, \tag{3}$$

where α is the angle between the vectors and $|\mathbf{x}|$ is the norm (1). Thus the angle between two vectors can be computed as:

$$\alpha = \arccos\frac{\mathbf{x}\cdot\mathbf{y}}{|\mathbf{x}||\mathbf{y}|} \,. \tag{4}$$

In general,

$$\mathbf{x}\cdot\mathbf{y} = \sum_{i=1}^{n} x_i y_i \,. \tag{5}$$

So the Spectral Angle Mapper (SAM) can be computed as follows:

$$\alpha = \arccos\frac{\sum_{i=1}^{n} x_i y_i}{\sqrt{\sum_{i=1}^{n} x_i^2}\sqrt{\sum_{i=1}^{n} y_i^2}} \,. \tag{6}$$

Notice that all elements x_i of spectral vectors are non-negative ($x_i \geq 0$), thus the spectral vectors [1] lie inside the positive cone of R^n.

The mutual angles among the spectral vectors (representing the three selected materials from Fig. 4) are drawn in Fig. 6. Fig. 4 shows that the shape of beech curve is more rugged than the shape of two other curves (dry clay and sand). Likewise, both angles between beech and dry clay or between beech and sand are significantly greater than the angle between similar smooth curves of dry clay and sand, as it is seen in Tab. 2. Therefore we looked for the answer, if the SAM can be reliably utilized for the recognition of pure spectra.

4. Analysis

To find the answer for the stated question and to verify the robustness of the SAM, we have modelled the endmembers loaded by different types of error as a simulation of suspicious conditions during the HSI datacube being recorded. The error loaded endmembers then has been compared with the pure spectra.

The surveillance devices utilized in the Army, as well as HSI devices, usually use visible (VIS) or infrared (IR) spectral region, alternatively both. Therefore the analysis has been aimed at these three regions and has been processed separately for VIS region (400 nm – 800 nm), IR region (800 nm – 2500 nm) and finally for full region VIS+IR (400 nm – 2500 nm). The goal was to find out if there are significant

differences among the results associated with respective spectral regions and additionally what regions are preferable to use for which kind of material.

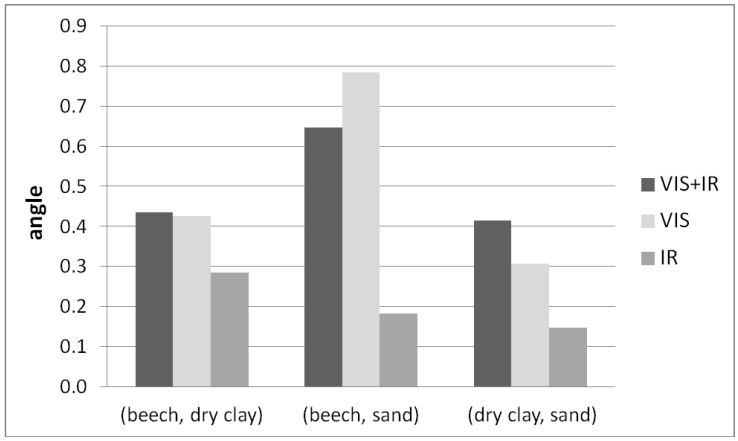

Fig. 6 Angles among spectral vectors of chosen materials

The spectra have been normalized for the processing, so the curves at their maximal elements are equal to one. The normalization of spectra allows partial eliminating some effects of conditions under which the HSI datacube was recorded.

The first analysis deals with the influence of additive noise with normal distribution characteristics. The error loaded vector has been computed, that for any element:

$$y_i = x_i[1 + k\,\mathrm{rand}(0, 1)], \tag{7}$$

where the rand (0, 1) is normally distributed pseudorandom number with $\mu = 0$ and $\sigma = 1$, x_i is the element of pure spectrum, k is the relative error; $k \in (0, 1)$. $k = 0$ means that there is no added noise and $k = 1$ means that the added relative error is equal to 100 % of measured value (value of element of vector of pure spectrum). The example of the original pure spectra and noise loaded signal is presented in Fig. 7a. The 10% additive signal has been superimposed on the pure spectrum of the beech. Both pure and noise loaded spectra are subsequently processed as a normalized signal. Thus the signals are normalized so the curve at its greatest element is equal to one. Normalized signals of both pure and noise loaded signals of beech from Fig. 7a are presented in Fig. 7b. The resulting angle between the spectral vectors of pure and noise loaded beech spectra of the example of 10% noise signal ratio is $\alpha = 0.096$.

The result of the analysis of superimposed noise for all three kinds of materials is presented in Fig. 8 which shows that the influence of additive noise is almost the same for any kind of material, as well as for any spectral region. It can be interpreted from the analysis that for up to 10 % of noise signal ratio, the angle between pure and noise loaded signal is less than 0.1. In accordance with the data in Fig. 6, the angle up to 0.1 allows suitable recognition of the kind of material.

The second analysis is focused on the influence of offset and degree of modulation. This analysis models the situation when the mean value of the error loaded signal arises along with the holdback of maximal value of original. The error loaded vector has been computed, that for any element:

$$y_i = r\,m(1 - x_i) + m x_i\,, \tag{8}$$

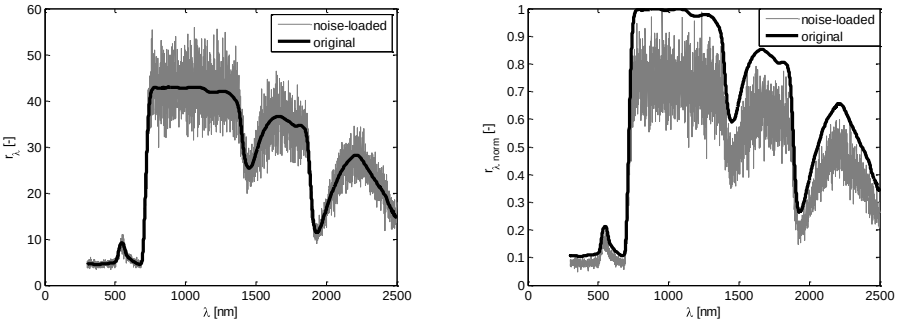

a) *b)*

Fig. 7 a) Original pure spectrum of beech and noise loaded signal with relative error 10 %, b) Normalized pure and noise loaded spectra of beech with relative error 10 %

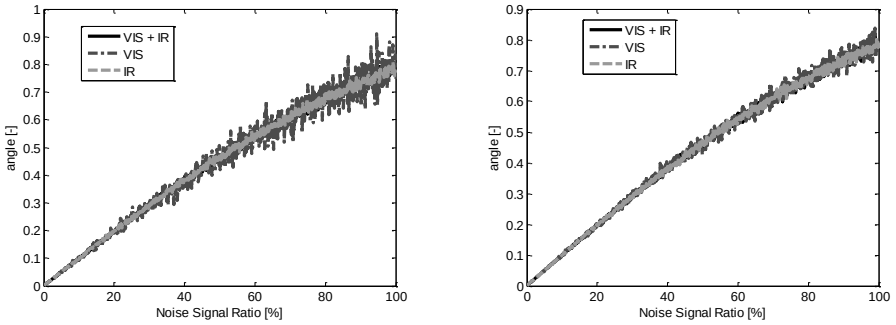

a) beech *b) dry clay*

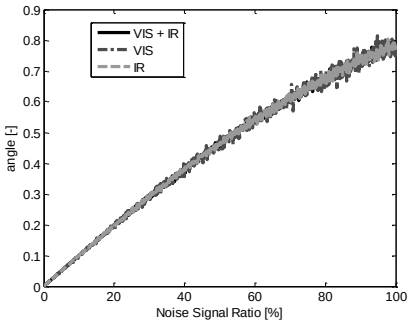

c) sand

Fig. 8 Differential angle between pure spectrum and noise loaded spectrum as a function of signal noise ratio in all three inspected regions VIS, IR, VIS+IR: a) beech, b) dry clay, c)sand

where r is the relative value of offset; $r \in (0, 1)$. $r = 0$ means that there is no added offset and $r = 1$ means that the added offset is equal to maximal measured value (value

of element of vector of pure spectrum), m is the maximal element of **x**; $m \in \mathbf{x}$, $m \geq x_i$ for any $x_i \in \mathbf{x}$. The example of the original pure spectra and offset loaded signal is presented in Fig. 9a. The pure spectrum of the beech has been superimposed on the 30% offset with appropriate decreasing of modulation. Both pure and offset loaded spectra are subsequently processed as a normalized signal. Thus the signals are normalized so the curve at its greatest element is equal to one. Normalized signals of both pure and offset loaded signals of beech from Fig. 9a are presented in Fig. 9b. The resulting angle between the spectral vectors of pure and offset loaded beech spectra of the example of 30% offset is $\alpha = 0.17$.

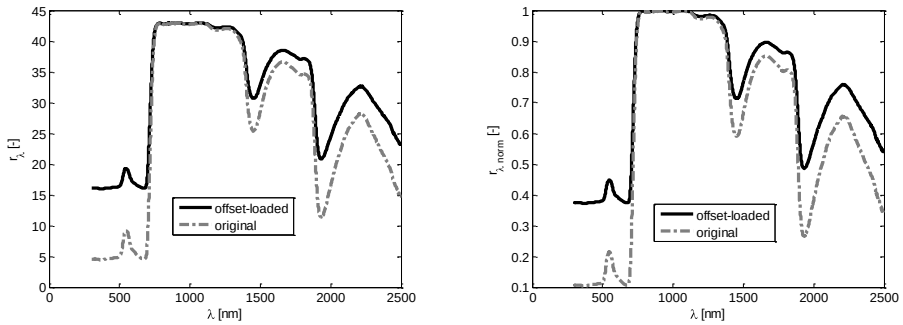

a) *b)*

Fig. 9 a) Original pure spectrum of beech and noise loaded signal with relative offset 30 %, b) Normalized pure and noise loaded spectra of beech with relative offset 30 %

The result of the analysis of superimposed offset with appropriate decreasing of modulation for all three kinds of materials is presented in Fig. 10. This figure shows that the influence of offset is significantly different in the different spectral region, as well as in different kinds of material. The analysis implies that the less modulated spectral curve, the lower influence of the offset. Thus the sand is at least sensitive on the offset and on the contrary, the beech is the most sensitive. Otherwise, it is valid for all three materials that the offset causes modification of vector angle in ascending order like this: IR, VIS+IR and VIS. If the angle 0.1 is taken again as a threshold for acceptable angle modification, the result for IR spectral region – 30% offset is acceptable for the beech, 70% is acceptable for dry clay and finally not even 100% offset causes the threshold angle modification.

The third and last analysis studies the influence of slant offset. It models the situation when the original signal is superimposed on the line with positive or negative slant. The error loaded vector has been computed, that for any element in the case of positive slant:

$$y_i = \frac{ms}{\lambda_{\max}} x_i (1 - x_i) + m x_i , \tag{9}$$

and in the case of negative slant:

$$y_i = (1 - x_i)\left(\frac{ms}{\lambda_{\max}} x_i + |ms| \right) . \tag{10}$$

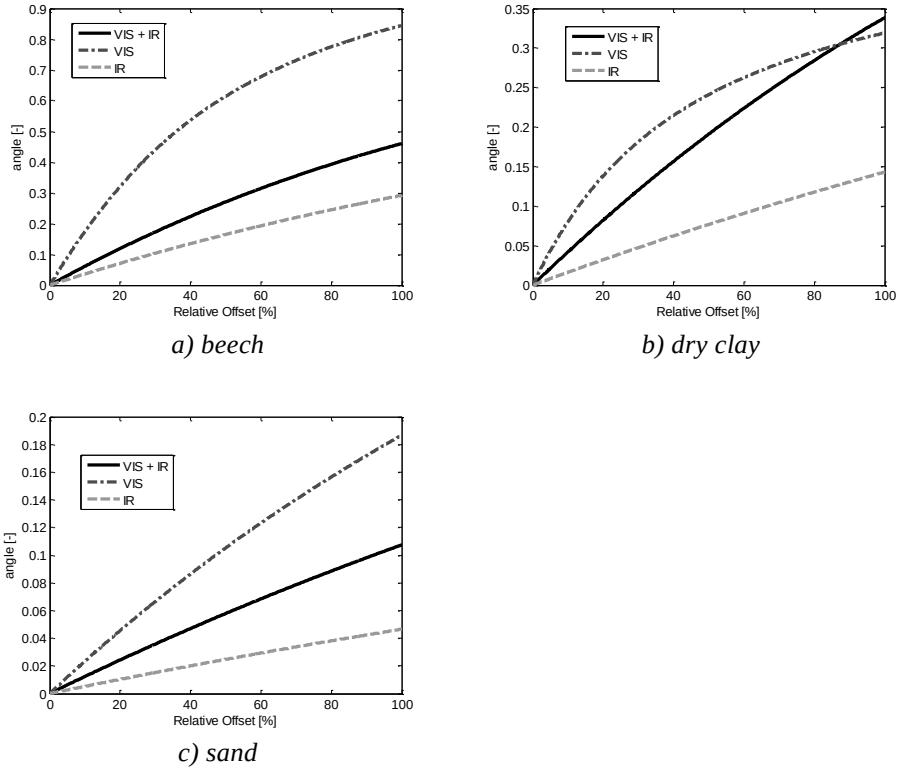

a) beech *b) dry clay*

c) sand

Fig. 10 Differential angle between pure spectrum and offset loaded spectrum as a function of relative offset with appropriate decreasing of modulation in all three inspected regions VIS, IR, VIS+IR: a) beech, b) dry clay, c)sand

where $|x|$ means magnitude (absolute value) of x, s is the relative slant; $s \in (-1, 1)$. $s = 0$ means that there is no added slant offset and $s = 1$ means that the pure spectrum is superimposed on the slant offset that is increasing with increasing wavelength and maximal value of the slant offset is equal to maximal value of the pure spectrum. This is analogically valid for $s = -1$, but the slant is reverse, so the slant offset is decreasing with increasing wavelength. λ_{max} is the maximal applied wavelength. The example of the original pure spectra and slant offset loaded signal is presented in Fig. 11a. The pure spectrum of the beech has been superimposed on the +50% slant offset. Both pure and slant offset loaded spectra are subsequently processed as a normalized signal. Thus the signals are normalized so the curve at its greatest element is equal to one. Normalized signals of both pure and slant offset loaded signals of beech from Fig. 11a are presented in Fig. 11b. The resulting angle between the spectral vectors of pure and slant offset loaded beech spectra of the example of +50% slant offset is $\alpha = 0.15$.

The result of the analysis of superimposed slant offset for all three kinds of materials is presented in Fig. 12. Although the resulting curves seem to be considerably different from the resulting curves of the offset (see Fig. 10), the effect is almost the same. It can be interpreted as the same result from the analysis: the less modulated spectral curve, the lower the influence of the slant offset. Similarly, the

sand is least sensitive on the offset and the beech is the most sensitive, and the spectral region responsibility on slant offset in ascending order: IR, VIS+IR and VIS. Additionally, there are ambiguous results when we compare the influence of the positive and negative slant. If, for the beech, in VIS region the influence of positive and negative slant is almost the same, so for the IR region the influence of positive slant is much more significant. On the contrary, in the case of dry clay the influence of negative slant is much more significant for VIS region, whereas in the case of IR region the influence of slant is almost the same for both negative and positive courses. Practically insignificant is the influence of slant offset for the sand. Except the negative slant for VIS region, the influence of slant offset is under the threshold angle 0.1 for the whole range of the slant.

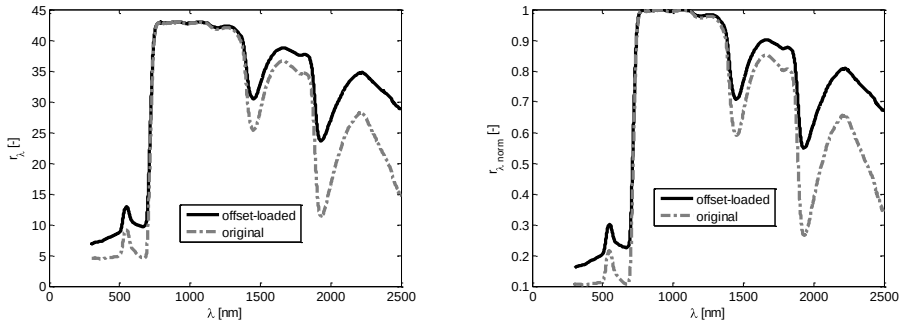

a) *b)*

Fig. 11 a) Original pure spectrum of beech and slant offset loaded signal with relative slant +50 %, b) Normalized pure and noise loaded spectra of beech with relative slant +50 %

5. Conclusion

It has been verified by the analysis that Spectral Angle Mapper (SAM) is a robust and reliable tool for matching the endmembers with pure spectra. It has also been found that the IR spectral region seems to be less sensitive for the influence of inspected effects, i.e. additive noise, constant offset and slant offset. On the other hand, the VIS region that seems to be the most sensitive for the effect's influence is more suitable for the respective matching. Both results follow from the shape of the spectral curves. The spectral curves of selected materials are more different in VIS region; therefore this region is more suitable for respective matching. However, due to the same reason this region is more sensitive for the influence of inspected effects.

References

[1] MANOLAKIS, D., MARDEN, D. and SHAW GA. Hyperspectral Image Processing for Automatic Target Detection Applications. *Lincoln Laboratory Journal*, 2003, vol. 14, no.1 p. 79-166. [cited 2012-07-09] Available from: <http://www.ll.mit.edu/publications/journal/pdf/vol14_no1/14_1hyperspectralprocessing.pdf>.

[2] GRAHN, HF. *Techniques and Application of Hyperspectral Image Analysis*. Wiley, 2007. 368 p.
[3] U.S. patent No. 7 336 353 (2008) *Coding and modulation for hyperspectral imaging*.
[4] BALÁŽ, T. *The Library of optical characteristics of mines and natural materials disposable in hyperspectral imaging* (in Czech) [Report of project SANDA]. Brno: VTÚO, 2011, 50 p.
[5] DEBBA, P. Field Sampling Scheme Optimization Using Simulated Annealing. In Chibante, R.(ed.) *Simulated Annealing, Theory with Applications*. Rijeka: InTech, Rui Chibante (Ed.), , InTech, 2010. ISBN 978-953-307-134-3. [cited 2012-07-09]. Available from: <http://www.intechopen.com/books/simulated-annealing--theory-with-applications/field-sampling-scheme-optimization-using-simulated-annealing>.

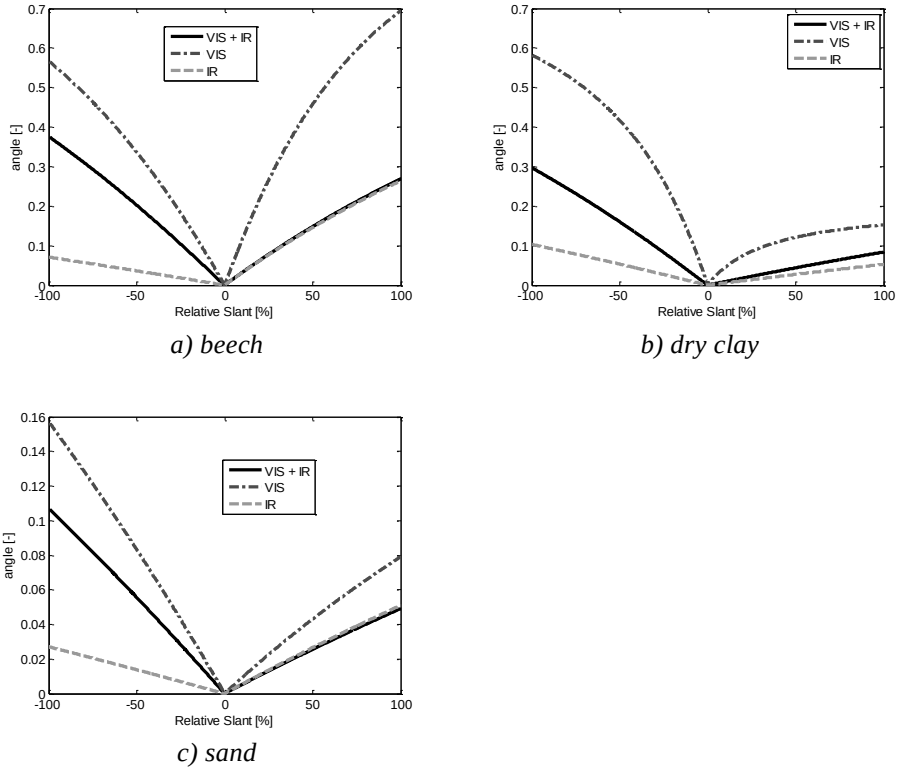

Fig. 12 Differential angle between pure spectrum and slant offset loaded spectrum as a function of relative slant offset in all three inspected regions VIS, IR, VIS+IR: a) beech, b) dry clay, c)sand

Acknowledgement

The work presented in this paper has been supported by the Ministry of Defence of the Czech Republic (research project PRO K201).